



Title	Probabilistic determination of pilot points for zonal voltage control
Authors(s)	Amraee, Turaj, Soroudi, Alireza, Ranjbar, AliMohammad
Publication date	2012-01
Publication information	Amraee, Turaj, Alireza Soroudi, and AliMohammad Ranjbar. "Probabilistic Determination of Pilot Points for Zonal Voltage Control." Institute of Engineering and Technology (IET), January 2012. https://doi.org/10.1049/iet-gtd.2011.0334 .
Publisher	Institute of Engineering and Technology (IET)
Item record/more information	http://hdl.handle.net/10197/6203
Publisher's statement	This paper is a postprint of a paper submitted to and accepted for publication in IET Generation, Transmission and Distribution and is subject to Institution of Engineering and Technology Copyright. The copy of record is available at IET Digital Library
Publisher's version (DOI)	10.1049/iet-gtd.2011.0334

Downloaded 2026-05-02 00:27:29

The UCD community has made this article openly available. Please share how this access benefits you. Your story matters! (@ucd_oa)



© Some rights reserved. For more information

Scenario-Based Selection of Pilot Nodes for Secondary Voltage Control

Turaj Amraee^{1*}, Alireza Soroudi¹, and AliMohammad Ranjbar¹

¹Department of Electrical Engineering, Sharif University of Technology, Tehran, Iran

Abstract—Due to local nature of the voltage and reactive power control, the voltage control is managed in a zonal or regional basis. In this paper a new comprehensive scheme for optimal selection of pilot points is proposed. The uncertainties of operational and topological disturbances of the power system are included to provide the robustness of the pilot node set. To reduce the huge number of probable states (i.e. combined states of load and topological changes) a scenario reduction technique is used. The resulted optimal control problem is solved using a new Immune-based Genetic Algorithm. The performance of the proposed method is verified over IEEE 118-Bus and realistic Iranian 1274-Bus national transmission grids.

Index Terms—Secondary voltage control, uncertainty, pilot node, scenario reduction, Immune-based Genetic Algorithm.

NOMENCLATURE

N_g	Number of generators or dynamic Var devices
N_l	Number of load buses
N_p	Number of pilot nodes
N_s	Number of combined load and contingency states
l_i	Subscribe stands for i^{th} load state
d_i	Subscribe stands for i^{th} contingency state
π_{d_i}	Probability of occurring of d_i^{th} contingency state
π_{l_i}	Probability of occurring of l_i^{th} load state
π_c	Probability of each combined state
l_n	Number of load states
d_n	Number of contingency states
m_j	Weighting factor for the j^{th} dynamic Var resource
r	Factor reflecting the order of the index for removing the masking effect in contingency screening
ΔQ_G	Vector of reactive power generation deviations
ΔQ_L	Vector of reactive power load perturbations
$\Delta Q_{L_{l_i}}$	Vector of reactive power load perturbations at l_i^{th} load state
ΔV_L	Voltage deviation at load buses
ΔV_P	Voltage deviation at pilot nodes
ΔV_G	Voltage deviation at generator stations
S_{GL}	Sensitivity matrix describing changes of reactive power at generator nodes w.r.t voltage magnitude changes at load buses
S_{GG}	Sensitivity matrix describing changes of reactive power at generator nodes w.r.t their voltage adjustment
S_{LG}	Sensitivity matrix describing changes of reactive power at load buses w.r.t voltage magnitude changes

	at generator nodes
P	Binary pilot node matrix denotes the location of pilot nodes among load buses
RSI_i	Reactive Support Index for i^{th} contingency
Q_{ji}^{no}	The unlimited reactive generation of the j^{th} dynamic Var device after contingency i
Q_j^{no}	The unlimited reactive generation of the j^{th} dynamic Var device in the pre-contingency case
PI_c	Performance index for c^{th} combined state
K_{svc}	Gain of linear feedback controller to maintain voltage magnitudes at pilot nodes
D_{ij}	Electrical distance between node i and j
R	Weighting factor to merit voltage control at some load buses

I. INTRODUCTION

A. Motivation And Problem Description

Voltage control could be carried out in a hierarchical way to obtain different goals at different layers. Due to local nature of the voltage and reactive power control, the voltage control is carried out in a regional or zonal basis. In other words, voltage control is performed in different hierarchical layers: primary layer, secondary layer and tertiary layer. The primary voltage control contains local automatic actions such as Automatic Voltage regulators of generators to diminish fast local disturbances (e.g. short circuits). Voltage magnitude is deviated from the desired thresholds by slow load perturbations. Therefore a secondary or zonal voltage control is needed to counteract slow variations of voltage magnitudes inside an electric region. The voltage magnitudes of load points could be controlled by dynamic reactive power resources. Therefore in addition of voltage control of load points it is needed to fair distribution or dispatch of the required reactive power among available resources. In other words, the zonal voltage control is designed to control the voltage magnitudes throughout the electric zones and fair distribution of required reactive power among available resources simultaneously. The time constant of the zonal or secondary voltage control is chosen more than the time constant of the primary control to insure the independency of the hierarchical control layers [1]. The whole grid is separated into distinct areas. Each electric area is represented by a pilot node and some regulating generators. The pilot node is a load point that its voltage magnitude has the maximum similarity to the area voltage profile. According to Fig. 1 by measuring voltage magnitude deviation at the pilot nodes the area's reactive power requirement is calculated

* Correspondence to: Turaj Amraee, Department of Electrical Engineering, Sharif University of Technology, Tehran, Iran, e-mail: (amraee@g2elab.grenoble-inp.fr).

by a proportional-integral law. Based on the output of this regulator a zone signal is obtained. Considering the zone signal all regulating generators inside a region will participate in voltage control with the same percentage of reactive power generation. The locations of pilot nodes has a major role in secondary voltage control performance. The optimal pilot node set obtained for a base case configuration cannot be optimal over the all possible operating scenarios. Thus, it is needed to improve the pilot node selection algorithms to make them robust against the uncertainties due to structural or operational changes in actual power system. This need motivates the work reported in this paper.

B. Literature Review

Various approaches have been proposed for pilot node selection problem including heuristic methods [2]–[6] and evolutionary optimization-based methods [7], [8]. In [2], the load buses with higher values of short circuit capacity are selected as pilot nodes. The concept of electrical distance in combination with clustering techniques is the next proposed method [3]. The pilot point selection could be formulated as an optimization model. The objective of this optimization problem is minimizing the voltage deviation throughout all electrical regions under all possible structural or load disturbances. The generator terminal voltage is taken as control variable. Two different approaches have been proposed to solve the optimization model: heuristic methods [4]–[6] and evolutionary technique [7], [8]. Recently some coordinated secondary voltage control schemes have been proposed to improve voltage stability margin or eliminate voltage violations. These scheme assume that the pilot nodes and associated control zones are known [9]–[12]. In [13] two very promising wide-area voltage protection (V-WAP) solutions, able to face stability and security problems in the transmission grid, have been presented with considering operation of secondary and tertiary control schemes according to their hierarchies. The major weakness of the previously proposed methods is the lack of robustness of the set of pilot nodes against structural (i.e. line or generator outages) and operational (i.e. load perturbations) changes in actual power system.

C. Contributions

Any secondary voltage control scheme should satisfy the following requirements:

- 1) R1: The voltage magnitude of the pilot node should represent the voltage profile of its associated region
- 2) R2: The regulating generators at each region should be able to provide enough reactive power support to regulate the voltage changes inside the region
- 3) R3: Each secondary voltage control area should be electrically decoupled from the other control areas
- 4) R4: The set of pilot nodes should be robust against the uncertainties due to structural or operational changes in actual power system

The gap that this paper intends to fill, is the consideration of fourth requirement in addition to the other three requirements.

Regarding this issue the uncertainties of loading conditions and the outages of main inter-area transmission lines are taken into account. The independency of the electrical zones is provided using the concept of electrical distance. To reduce the computational burden of the problem and uncertainty modeling a scenario reduction technique is developed. The pilot selection problem is a mixed integer nonlinear optimization problem. Therefore, in this paper, a new hybrid Immune-Genetic Algorithm is proposed to solve the optimal pilot node selection problem.

D. Paper Organization

The rest of this paper is organized as follows. In section 2, the detailed formulation of the secondary voltage control is presented. The proposed evolutionary algorithm is described in Section 3. In Section 4 the proposed scheme will be simulated for IEEE 118-Bus test system and a large scale realistic transmission network (Iranian 1274-Bus national grid). The conclusions are given in section 5.

II. PILOT NODE SELECTION FORMULATION

The overall structure of the multilayer voltage control is shown in Fig. 1. By measuring the voltage deviation at pilot point a zone signal, i.e. N , is obtained using a proportional integral controller. The zone signal forces all regulating generators to have the same participations in voltage control (i.e. same percentages of reactive power generation). Using the decoupled power flow model of the steady state system equations the linearized model of the zonal voltage control could be formulated via (1)-(3).

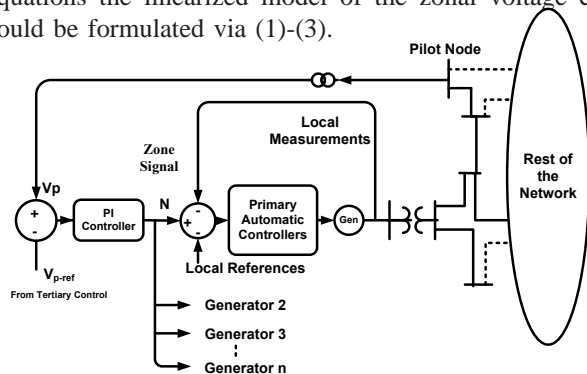


Fig. 1. Block diagram of the secondary voltage control scheme

$$\begin{bmatrix} \Delta Q_G \\ \Delta Q_L \end{bmatrix} = \begin{bmatrix} S_{GG} & S_{GL} \\ S_{LG} & S_{LL} \end{bmatrix} \begin{bmatrix} \Delta V_G \\ \Delta V_L \end{bmatrix} \quad (1)$$

$$\Delta V_L = J_1 \Delta Q_L + J_2 \Delta V_G \quad (2)$$

where

$$J_1 = S_{LL}^{-1} J_2 = -S_{LL}^{-1} S_{LG} \quad (3)$$

Due to hierarchical nature of the SVC, the primary control is reached its steady state before the initiation of the secondary layer and so on. The lack of sufficient measurement and communication infrastructures at all load buses necessitates the existence of a minimum number of pilot nodes that their measurements are sufficient to control the voltage profile over all electrical zones. A linear controller in which the initial post-contingency pilot node voltage deviations written as a function of the set-point changes of regulating units is formulated as follows.

$$\Delta V_G = K_{svc} \Delta V_L^0 \quad (4)$$

where ΔV_L^0 denotes voltage deviation at load buses without secondary control. The voltage magnitudes are measured only at pilot nodes:

$$\Delta V_P = P \Delta V_L^0 \quad (5)$$

$$\Delta V_G = K_{svc} \Delta V_P = K_{svc} P J_1 \Delta Q_L \quad (6)$$

The pilot node matrix is defined as follows.

$$P = [p_{ij}]_{N_p \times N_l} \quad (7)$$

$$p_{ij} = \begin{cases} 1 & \text{if bus } i \text{ is the } j^{\text{th}} \text{ pilot node} \\ 0 & \text{otherwise} \end{cases} \quad (8)$$

The voltage deviation of load points could be defined as a function of controller gain, K_{svc} , and pilot node matrix, P, as follows.

$$\begin{aligned} \Delta V_L &= J_1 \Delta Q_L + J_2 K_{svc} P J_1 \Delta Q_L \\ &= (I + J_2 K_{svc} P) J_1 \Delta Q_L \end{aligned} \quad (9)$$

The objective function or performance index of the secondary control scheme, PI , could be defined as the total weighted sum of squares of voltage deviations throughout the network. For a given load disturbance given by ΔQ_L , it could be formulated via (10)-(13).

$$PI = (\Delta V_L)^T . R . (\Delta V_L) \quad (10)$$

$$PI = \text{trace}[R . (I + J_2 K_{svc} P) G (I + J_2 K_{svc} P)^T] \quad (11)$$

where

$$G = (J_1) \Lambda (J_1)^T \quad (12)$$

$$\Lambda = (\Delta Q_L) (\Delta Q_L)^T \quad (13)$$

A. Uncertainty Modeling

The selected pilot nodes should provide a desired level of robustness against load and contingency uncertainties. In this section, a general procedure is proposed to model the uncertainties of load perturbations and structural changes (i.e.outages).

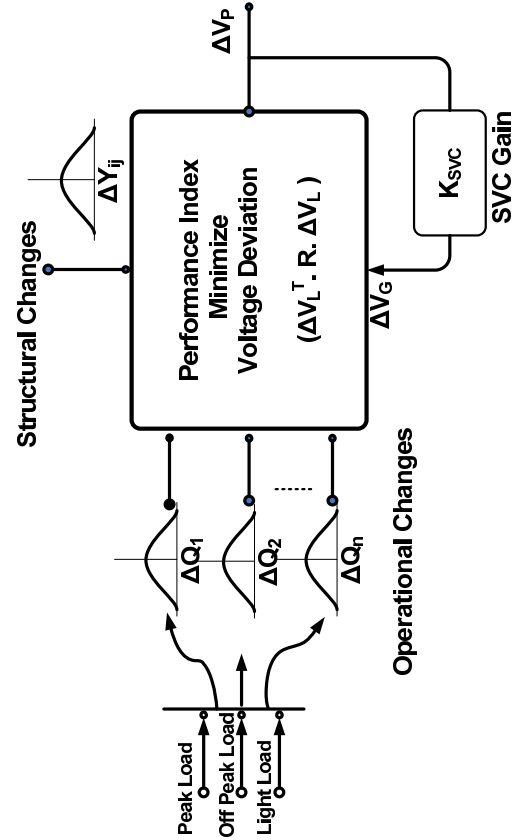


Fig. 2. Operational and Structural uncertainty of secondary voltage control

1) *Load Uncertainty Modeling*: In fact, the load disturbance has a random nature and so the performance index is a random variable. Therefore, to consider this randomness, the deterministic performance index should be replaced by a probabilistic index. Here, three load levels have been considered : Peak-Load, Off-Peak Load, and Light Load. The load perturbation around each load level has a normal distribution as shown in Fig. 2. The load will be divided into different levels using a clustering technique, utilizing the central centroid sorting process. All these states are defined as a percentage of the base-case loading. Mathematically each load state i.e. l_i , is described with its ΔQ_{l_i} and probability of occurrence, i.e. π_{l_i} .

2) *Topological Uncertainty Modeling*: The outage(i.e. topological changes) modeling is carried out in two consequent steps. In the first step the contingency screening is done and the contingency modeling will then be followed in the second step.

- **Contingency Screening**: The most credible contingencies should be screened and weighted based on their probabilities. Reactive Support Index (RSI) proposed in [14], has been used for contingency ranking based on the capability of the power system in voltage and reactive power support. The RSI index, for a given contingency, is defined as the additional amount of reactive generation required to get from the base-case saddle-node point to the contingency nose-point. The Reactive Support Index is defined as the extra amount of reactive generation from all the existing dynamic VAR resources (e.g. generation, SVC, etc.) in which the reactive limits at the dynamic VAR devices are removed [14].

$$RSI_i = \sum_{j=1}^{N_g} m_j (Q_j^{no} - Q_{ji}^{no})^r \quad (14)$$

where RSI_i is the relative RSI index for contingency i . Q_j^{no} and Q_{ji}^{no} are calculated with open reactive limits of dynamic Var devices [14].

- Contingency States After carrying out contingency analysis, in the first stage, a list of the most critical contingencies are selected. In the second stage, based on the forced outage rate or other historical information, the probability of each screened contingency is calculated. Here, without losing generality, only the severe contingencies are selected based on the value of RSI index calculated in (14). In this paper, only the outages of tie-line transmission lines are taken into account. The normal state is considered as a state in which all equipments are in-service. Mathematically each contingency state i.e. d_i , is described with its RSI_i and probability of occurrence, i.e. π_{d_i} .

B. Combined Load and Contingency States

It is assumed that the load and contingency states are independent so the states are combined to construct the whole set of states as follows:

$$\pi_c = \pi_l \times \pi_d \quad (15)$$

The total number of states, i.e., N_s , will be $l_n \times d_n$. For a large scale power system the huge number of scenarios (i.e. states) will increase the computational burden of the optimization task, enormously. In this paper a scenario reduction technique is implemented to reduce the total number of scenarios without losing much information of the original set of scenarios. The scenario reduction technique has been used in risk-averse decision making [15] and electricity market [16]. The formulation of the scenario reduction technique could be found in Appendix.

For uncertainty modeling the performance index could be formulated via (16) to (19).

$$PI = \sum_{c=1}^{N_s} \pi_c PI_c \quad (16)$$

$$PI = \text{trace}[R.(I + J_{2c}K_{svc}^c P)G_c(I + J_{2c}K_{svc}^c P)^T] \quad (17)$$

where

$$G_c = (J_{1c})\Lambda_c(J_{1c})^T \quad (18)$$

$$\Lambda_c = (\Delta Q_{Lc})(\Delta Q_{Lc})^T \quad (19)$$

C. Optimal Gain

For a given pilot matrix, P , the controller gain, K_{svc} , is optimized with any integral control law, provided that the gain matrix, K_{svc}^c verifies (4). The optimal gain of controller could be determined by two different strategies. In the first strategy the total voltage deviation over all load buses is

minimized without minimizing voltage changes of regulating units, while in the second one the voltage deviation of pilot nodes is forced to be zero by minimizing voltage changes of regulating units. The optimal gain of linear controller for both strategies for each combined state is determined via (20) and (21), respectively.

$$\begin{aligned} \frac{\partial PI_c}{\partial K_{svc}} = 0 &\Rightarrow \\ K_{svc}^* &= [J_{2c}^T R J_{2c}]^{-1} J_{2c}^T R G_c P^T [P^T R P]^{-1} \end{aligned} \quad (20)$$

$$\Delta V_P = 0 \Rightarrow K_{svc}^* = [P J_{2c}]^{-1} (P^T J_{2c}^T J_{2c} P)^{-1} \quad (21)$$

D. Optimization problem

1) *Constraints*: Many constraints could be included in the pilot selection problem. Here, two main constraints are included to provide the independency of pilot nodes and to respect the limits of reactive power generations and terminal voltage changes of generators as well as voltage deviation of pilot nodes after implementing control actions. To provide the independency between electrical zones or pilot nodes, each two pilot pair should have a minimum electrical distance as follows.

$$D_{ij}^c = -\text{Log}(\alpha_{ij}^c \times \alpha_{ji}^c) \quad i, j \in 1, \dots, n_l \quad (22)$$

$$\alpha_{ij}^c = \frac{\partial V_i / \partial Q_j}{\partial V_j / \partial Q_i} \quad i, j \in 1, \dots, n_l \quad (23)$$

2) *Optimization Problem*: By considering all probable scenarios of loading conditions and topological changes of the network, the optimal pilot set is the one that has the minimum cost for all loading conditions over the base-case and contingency configurations. Therefore the PI is rewritten to consider all load and network states as follows.

$$\min_P PI = \sum_{c=1}^{N_s} \pi_c PI_c \quad (24)$$

subject to

$$PI_c = \quad (25)$$

$$\text{trace}[R.(I + J_{2c}K_{svc}^c P)G_c(I + J_{2c}K_{svc}^c P)^T]$$

$$K_{svc}^c = \quad (26)$$

$$\begin{cases} [J_{2c}^T R J_{2c}]^{-1} J_{2c}^T R G_c P^T [P^T R P]^{-1} & 1^{st} \text{ law} \\ P J_{2c}^{-1} P^T J_{2c}^T N_S P & 2^{nd} \text{ law} \end{cases}$$

$$D_{ij}^c \geq D_{ij}^{min} \quad (27)$$

$$\Delta V_{Gmin}^c \leq \Delta V_G^c \leq \Delta V_{Gmax}^c \quad (28)$$

$$\Delta Q_{Gmin}^c \leq \Delta Q_G^c \leq \Delta Q_{Gmax}^c \quad (29)$$

$$\Delta V_{Lmin}^c \leq \Delta V_L^c \leq \Delta V_{Lmax}^c \quad (30)$$

where $\Delta Q_G^c, \Delta V_G^c$, and ΔV_L^c are determined via (1), (5), and (9). Indeed due to the random natures of load and topological disturbances the secondary voltage control is a stochastic mixed integer non-linear optimization problem. In this paper, an Immune-GA-Based Technique is proposed to solve the optimization problem.

III. PROPOSED IMMUNE-GA METHOD

Immune Algorithm is a heuristic method which imitates the human's reaction against external invasions. This algorithm has been successfully applied to pattern recognition [17] and multi-objective DG planning problem [18], [19]. In Immune algorithm, the objective functions and their associated constraints are assumed to be antigens and the solutions act as antibodies. Affinity factors are defined as the ability of antibodies (solutions) in recognizing (optimizing) the antigens (objective functions and constraints). Immune algorithm it is an iterative methodology which starts with an initial set of solutions and improves its performance. The Immune algorithm has two important operators namely, cloning and mutation [19]. The cloning operator reproduces the antibodies with a change proportional to their ability in recognizing the antigens (affinity) [19], [20]. The mutation operator applies some perturbation on antibodies in hope to find better ones. The mutation probability is related to the inverse value of the affinities. In order to enhance the strength of the algorithm, crossover operator [21] of GA is proposed in the present work to overcome the lack of memory in immune algorithm. To do this, in the cloning phase, the algorithm selects two solutions (instead of one) and performs the crossover operation. It then generates two new solutions and passes them to mutation operator. Mutation operator uses the value of affinity factor of the selected parents (i.e. antigens) as a measure for mutating them. The proposed solution algorithm is described as the following steps:

- Step 1. Generate initial N_{pop} solutions
- Step 2. Set $Iteration = 1$
- Step 3. Calculate the objective function (affinity factor) for each antibody using (24)
- Step 4. If $Iteration \geq$ maximum number then end; else continue
- Step 5. Keep the best antibodies in memory
- Step 6. Set the cloning counter, i.e. m , equal to 1
- Step 7. Select two antibodies (p and q) as the parents among the antibodies stored in memory, using roulette wheel based on their affinities
- Step 8. Calculate the number of cloning replica, i.e. k_m , and mutation probabilities based on the average values of parent affinities. The value of k_m is determined as follows:

$$k_m = round(\Gamma \times \frac{OF_p + OF_q}{2max(OF_n)} \times N_{pop}) \quad (31)$$

Where, Γ is a controlling factor and $round$ is the function which gives the nearest integer number

- Step 9. Clone the selected parents selected in Step.7, for k_m times, by applying the crossover and mutation operators and produce new antibodies
- Step 10. Store the new generated antibodies
- Step 11. If the cloning counter is below the memory size, then increase cloning counter and go to Step.7 ; else, construct the new antibody set using the union of newly generated antibodies and the antibodies of memory, increase the iteration and go to Step.3

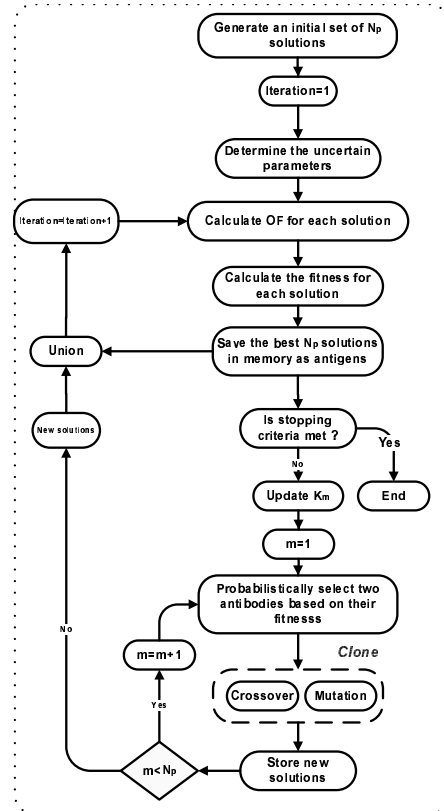


Fig. 3. The flowchart of the proposed method

IV. SIMULATION RESULTS

The proposed model is simulated over IEEE 118 Bus test case and the realistic 1274-Bus transmission grid of Iran. The obtained optimal patterns of pilot nodes are compared to previously proposed methods. It is assumed that all load buses are candidates to be selected as pilot node. The results of simulations are presented for the second control law. Solving the (24) gives $21(\text{contingency states}) * 10(\text{load states}) = 210$ states for IEEE 118 and $31(\text{contingency states}) * 10(\text{load states}) = 310$ for 1274-Bus Iranian grid. It is clear that the calculation process for all these states imposes a heavy computational burden. In order to overcome this problem, a scenario reduction technique is implemented to reduce the number of states (see Appendix for more details) [15].

A. Load States

Ten independent load levels are chosen based on the clustering technique and utilizing the central centroid sorting process [22]. The proposed method in [22] verifies that choosing ten equivalent load levels (states), with different probabilities π_{l_i} , provides a reasonable trade-off between accuracy and fast numerical evaluation. The states have been described as a fraction of base case loading as given in Table I. This load states are applied to both test cases without losing generality.

B. Contingency States

Contingency screening is carried out based on the value of RSI index as described before. The results of RSI calculations for both test cases are shown in Table II and Table III.

TABLE I
LOAD STATES AND THEIR PROBABILITIES

Load State	Load Perturbation (% of Base-Case)	Probability
1	20.00	0.0100
2	17.06	0.0560
3	15.48	0.1057
4	14.26	0.1654
5	13.00	0.1654
6	11.70	0.1630
7	10.20	0.1630
8	9.020	0.0912
9	8.120	0.0473
10	7.020	0.0330

TABLE II
CONTINGENCY STATES AND THEIR PROBABILITIES, IEEE-118 BUS SYSTEM

Contingency State	Configuration(from-to)	RSI Value	Probability
0	BC	0	0.9600
1	C1 (38 - 37)	7.227	0.002
2	C2 (8 - 5)	5.788	0.002
3	C3 (38 - 65)	4.688	0.002
4	C4 (69 - 75)	4.280	0.002
5	C5 (94- 100)	3.084	0.002
6	C6 (69 - 70)	2.533	0.002
7	C7 (26 - 30)	2.399	0.002
8	C8 (74 - 75)	2.342	0.002
9	C9 (100 -101)	2.200	0.002
10	C10 (88 -89)	2.085	0.002
11	C11 (3 - 5)	2.021	0.002
12	C12 (76 -77)	2.020	0.002
13	C13 (49 -50)	1.977	0.002
14	C14 (1 - 3)	1.931	0.002
15	C15 (30 -17)	1.917	0.002
16	C16 (2 - 12)	1.891	0.002
17	C17 (49 -51)	1.868	0.002
18	C18 (70 -74)	1.840	0.002
19	C19 (30 -38)	1.764	0.002
20	C20 (34 -37)	1.627	0.002

The 20 reduced states by using the scenario reduction technique are given in Table.IV and Table.V.

C. Case 1: IEEE-118 Bus test case

The proposed model is applied to IEEE-118 bus test case. The loading data of this test case are modified based on [23]. Generation units with low reactive power capacities are converted to load buses.

1) *IEEE-118 Bus Without Uncertainty Modeling*: For this case the number of population is assumed as $N_P = 50$. Other optimization parameters such as clonal factors, crossover and mutation rates are assumed adaptively. The results are given in Table. VI. The best objective function using the proposed method is compared with other heuristic and intelligent techniques. The optimal cost for the optimal pilot set is 0.9183×10^{-2} . According to the constraint of minimum electrical distance the obtained pilot locations are distributed throughout the network. To verify the overall performance of the obtained pilot nodes a load reactive power disturbance of 25% is applied to all the load buses. The voltage deviations for the first 40 load buses with highest deviations are shown in Fig. 4 for different pilot sets obtained by various methods. It

TABLE III
CONTINGENCY STATES AND THEIR PROBABILITIES, IRAN 1274-BUS SYSTEM

Contingency State	Configuration(from-to)	RSI Value	Probability	
C0	Base Case	-	0	0.940
C1	(BAM-NZAHDA)	(5040 - 4810)	18.186	0.002
C2	(RAJAG-AMIRK)	(3490 - 5340)	5.6370	0.002
C3	(BIRJ2-SEFIDA)	(3780 - 6080)	5.6256	0.002
C4	(TEHP1-DAMAV)	(3610 - 4760)	4.5605	0.002
C5	(TEHP2-DAMAV)	(3620 - 4760)	4.5605	0.002
C6	(ARAK-RUDES)	(1220 - 3530)	4.4085	0.002
C7	(NKER4 - BAM)	(4660 - 5040)	4.2578	0.002
C8	(SIRJA-GENOV4)	(2500 - 501)	3.8933	0.002
C9	(KANI-ZIARA4)	(3310 - 3660)	3.8392	0.002
C10	(FIBAH4-NRUD4)	(3170 - 4790)	3.7977	0.002
C11	(FIBAH4-NRUD4)	(3170 - 4790)	3.7977	0.002
C12	(TEHP14-TEHPS)	(3610 - 3630)	3.7165	0.002
C13	(TEHP24-TEHPS)	(3620 - 3630)	3.7165	0.002
C14	(JALAL-REYN4)	(3270 - 3520)	3.5904	0.002
C15	(GOTVA-AMIRK)	(4140 - 5340)	3.4666	0.002
C16	(YAZD-NCHLST)	(3970 - 4560)	3.0803	0.002
C17	(KATUN-YAZD14)	(2430 - 3950)	2.8604	0.002
C18	(GODAR4-GOLPA)	(4130 - 1530)	2.7743	0.002
C19	(YAZD-HARAND)	(3970 - 6470)	2.6365	0.002
C20	(FASA4 -BOTASL)	(1830 - 6140)	2.5073	0.002
C21	(CHOGH-OMID34)	(1780 - 7150)	2.1429	0.002
C22	(KHORM-KARKH)	(1310 - 4160)	2.1052	0.002
C23	(PARDI4-PARDI2)	(3440 - 3430)	2.0612	0.002
C24	(NCHLST-SORMIG)	(4560 - 4600)	1.8965	0.002
C25	(PARDI4-DAMAV)	(3440 - 4760)	1.7015	0.002
C26	(ZANJ24-IJRUD4)	(3030 - 7260)	1.6407	0.002
C27	(GARMS-SEMNA)	(3080 - 3090)	1.2975	0.002
C28	(PARDI4-PARKJ4)	(3440 - 3460)	1.0266	0.002
C29	(PARDI4-SADAT4)	(3440 - 3540)	0.6567	0.002
C30	(KHOR2-KHOR4)	(1300 - 1310)	0.2063	0.002

TABLE IV
TOTAL REDUCED STATES AND THEIR PROBABILITIES FOR IEEE 118-BUS TEST CASE

New State No	Original State No	Load State (% of BaseCase Load)	Contingency State (RSI value)	Probability
S1	1	20.00	0.000	0.00960
S2	22	17.60	0.000	0.05376
S3	40	17.60	1.840	0.00226
S4	43	15.48	0.000	0.10147
S5	62	15.48	1.764	0.00338
S6	64	14.26	0.000	0.15878
S7	82	14.26	1.840	0.00529
S8	85	13.00	0.000	0.15878
S9	87	13.00	5.788	0.00320
S10	103	13.00	1.840	0.00529
S11	106	11.70	0.000	0.15648
S12	109	11.70	4.688	0.00324
S13	117	11.70	2.021	0.00522
S14	127	10.20	0.000	0.15648
S15	128	10.20	7.227	0.00134
S16	145	10.20	1.840	0.00522
S17	148	09.02	0.000	0.08755
S18	169	08.12	0.000	0.04541
S19	183	08.12	1.931	0.00555
S20	190	07.02	0.000	0.03168

can be seen that the pilot set obtained by the proposed method provide better voltage profile over the grid.

2) *IEEE-118 Bus With Uncertainty Modeling*: In this case the load and contingency states are considered as given in Table. I and Table. II. The 20 reduced combined states are given in Table. VII. Choosing more than 20 reduced scenarios adds no significant gain for this case. The best objective function using the proposed method is compared with other techniques. To verify the effectiveness of the proposed method one of the combined states, S15, is applied to the system. The voltage deviation for first 40 load buses (i.e. buses with highest voltage deviations)are given in Fig. 5. It can be seen that the proposed method provides better voltage profile over the grid.

D. Case 2: Iranian National Transmission Grid

Iranian national transmission grid consists of 1274 nodes, 551 generation units and 724 load points. The standard transmission voltages are 400 kV and 230 kV. The 400 kV backbone is shown in Fig. 6. The load, contingency, and

TABLE V
TOTAL REDUCED STATES AND THEIR PROBABILITIES FOR IRAN
1274-BUS SYSTEM

New State No	Original State No	Load State (% of BaseCase Load)	Contingency State (RSI value)	Probability
S1	31	20.00	0.2063	0.00998
S2	32	17.60	0.0000	0.05421
S3	63	15.48	0.0000	0.10020
S4	80	15.48	2.8604	0.00654
S5	94	14.26	0.0000	0.15779
S6	103	14.26	3.8392	0.00770
S7	125	13.00	0.0000	0.15746
S8	135	13.00	3.7977	0.00397
S9	139	13.00	3.5904	0.00364
S10	156	11.70	0.0000	0.15452
S11	157	11.70	18.1860	0.00200
S12	172	11.70	3.0803	0.00815
S13	187	10.20	0.0000	0.15452
S14	206	10.20	2.6365	0.00896
S15	218	09.02	0.0000	0.08573
S16	220	09.02	5.6370	0.00156
S17	248	09.02	0.2063	0.00128
S18	249	08.12	0.0000	0.04541
S19	253	08.12	4.5605	0.00463
S20	280	07.02	0.0000	0.03175

TABLE VI
OPTIMAL PILOT NODES AND PERFORMANCE INDEX BY APPLYING THE
SECOND CONTROL LAW, 118-BUS SYSTEM

Solution Method	Optimal Pattern	Performance Index
Simulated Annealing [4]	12,17,23,39,56,68,71,77,92,103	1.1099×10^{-2}
Greedy Search [6]	14,77,92,38,56,103,23,47,71,60	1.1481×10^{-2}
Extended Greedy Search [6]	12,23,38,47,56,60,71,77,88,103	1.1399×10^{-2}
Immune Algorithm [8]	12,39,77,88,55,105, 47,28,71,15	1.0510×10^{-2}
Proposed Algorithm	11,20,30,38,63,70,77,86,93,108	0.9183×10^{-2}

reduced combined states are given in Table. I, Table. III, and Table. V. The obtained results are given in Table. VIII. The total 32 pilot points are given for each region with and without uncertainty modeling. Referring to the single line diagram of the Iranian National Grid it can be seen that the obtained results have been distributed throughout the network.

V. CONCLUSION

The previously proposed model of secondary voltage control was modified to take into account topological and operational disturbances. The optimization model as a full integer programming problem was solved using a new Immune-GA based algorithm which was robust and could find better solutions with low computational burden by considering load and structural uncertainty. To reduce the computational burden the total number of states was reduced by a scenario reduction technique. The proposed scheme was applied to IEEE 118-Bus test case and Iranian 1274-Bus transmission grid and the obtained results verified the robustness of the proposed method.

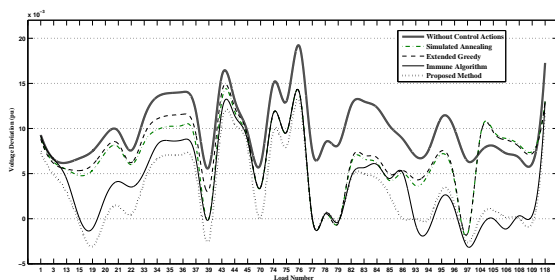


Fig. 4. Voltage deviation of load buses for different sets of pilot nodes without uncertainty modeling, 118-Bus system

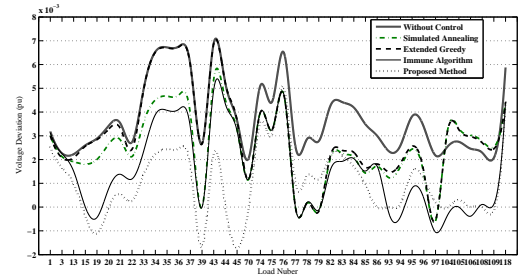


Fig. 5. Voltage deviation of load buses for different sets of pilot nodes with uncertainty modeling, 118-Bus system

TABLE VII
OPTIMAL PILOT NODES AND PERFORMANCE INDEX BY APPLYING THE
SECOND CONTROL LAW, 118-BUS SYSTEM WITH UNCERTAINTY
MODELING

Solution Method	Optimal Pattern	Performance Index
Simulated Annealing [4]	12,17,23,39,56,68,71,77,92,103	2.01019×10^{-4}
Greedy Search [6]	14,77,92,38,56,103,23,47,71,60	1.98944×10^{-4}
Extended Greedy Search [6]	12,23,38,47,56,60,71,77,88,103	2.02530×10^{-4}
Immune Algorithm [8]	12,39,77,88,55,105, 47,28,71,15	1.90971×10^{-4}
Proposed Algorithm	11,20,38,44,50,68,70,86,93,108	1.57271×10^{-4}

APPENDIX: SCENARIO REDUCTION TECHNIQUE

The purpose of scenario reduction is selection of a set, i.e. Ω_S , with the cardinality of N_{Ω_S} , from the original set, i.e. Ω_J [16]. This procedure should be done in a way that makes a trade off between the loss of the information and decreasing the computational burden [24]. The scenario reduction technique used in this paper is described as the following steps [15]:

step. 1 Construct the matrix containing the distance between each pair of scenarios $c(w, \hat{w})$

Fig. 6. Iranian National Transmission Grid (400 kV backbone)

TABLE VIII
OPTIMAL PILOT NODES AND PERFORMANCE INDEX FOR IRANIAN
1274-BUS NATIONAL TRANSMISSION GRID

Uncertainty Modeling	Region	Optimal Pilots	PI
Without Uncertainty	Azarbajjan	Miandoab-230	0.5024
	Bakhtar	Amirkabir-400	
	Isfahan	Tiran-400,Mobarake-230,Najafabad-400,Zobahan-400.	
	Fars	Fars-400, Asaluyeh-400	
	Gharb	EastKermansh-400	
	Gilan	GilanCC-230	
	Hormozgan	BandarAbbas-400	
	Kerman	Sirjan-400	
	Khorasan	Neyshabur-400, Tus-400, KohSangi-400	
	Khuzestan	Andimshk-230,Abaspour-400,Ahwaz-400,Godar-400,Gotvand-400	
	Mazandaran	Neka-400, AliAbad-400	
	Semnan	Ahuan-400	
	Tehran	Damavand-400, Jalal-400, RudShur-400,Ziaran-400,Pardis-400,Mosalla-230	
	Sistan	NZahedan-230	
Zanjan	Zanjan-400, SheykheBaha-400		
With Uncertainty	Azarbajjan	Tabriz 400	0.00875
	Bakhtar	Anjirak-400,Khoramabad-400,Amirkabir-400	
	Isfahan	NChelstun-400,Tiran-400,Golpayegan-400.	
	Fars	Asaluyeh-400,Fasa-400.	
	Gharb	EastKermansh-400	
	Gilan	NGilan-230	
	Hormozgan	Pyan-230, Almahdi-230,Geno-400	
	Kerman	ArgeBam-230	
	Khorasan	Sarakhs-400,Toos-400.	
	Khuzestan	Ahwaz22-230,Ahwaz4-400,Omidyeh-400,Godar-400,Sushtar-400,Gotvand-400	
	Mazandaran	Mindashi-230,Darys-230,Neka-400	
	Tehran	Damavand4-400,RudSur-400,FrüzBahram-230,Ziaran-400,Sheikh-400	
	Sistan	NZahedan-230,Polan2-230	

step. 2 Select the first scenario w_1 as follows:

$$w_1 = \arg \left\{ \min_{w' \in \Omega_J} \sum_{w \in \Omega_J} \pi_w c(w, w') \right\} \quad (32)$$

$$\Omega_S = \{w_1\}, \Omega_J = \Omega_J - \Omega_S$$

step. 3 Select the next scenario to be added to Ω_S as follows:

$$w_n = \arg \left\{ \min_{w' \in \Omega_J} \sum_{w \in \Omega_J - \{w'\}} \pi_w \min_{w'' \in \Omega_S \cup \{w'\}} c(w, w'') \right\} \quad (33)$$

$$\Omega_S = \Omega_S \cup \{w_n\}, \Omega_J = \Omega_J - \Omega_S$$

step. 4 If the number of selected set is sufficient then end and go to step 2 ; else continue.

step. 5 The probabilities of each non-selected scenario will be added to its closest scenario in the selected set.

step. 6 End.

REFERENCES

- [1] J. P. Paul, J. Y. Leost, and J. M. Tesson, "Survey of the secondary voltage control in france : Present realization and investigations," *Power Systems, IEEE Transactions on*, vol. 2, no. 2, pp. 505 –511, May 1987.
- [2] V. Arcidiacono, "Automatic voltage and reactive power control in transmission systems," *Power Delivery, IEEE Transactions on*, vol. Florence, no. IFAC Symp. on Power Systems, July 1983.
- [3] P. Lagonotte, J. Sabonnadiere, J.-Y. Leost, and J.-P. Paul, "Structural analysis of the electrical system: application to secondary voltage control in france," *Power Systems, IEEE Transactions on*, vol. 4, no. 2, pp. 479 –486, May 1989.
- [4] M. Ilic-Spong, J. Christensen, and K. Eichorn, "Secondary voltage control using pilot point information," *Power Systems, IEEE Transactions on*, vol. 3, no. 2, pp. 660 –668, May 1988.
- [5] P. Lagonotte, "Analyse structurale des réseaux électriques application au réglage hiérarchisé de la tension du réseau français," in *Cigre Task Force 38-02-08*, 1987, i.N.P., Grenoble.
- [6] A. Conejo, T. Gomez, and J. de la Fuente, "Pilot bus selection for secondary voltage control," *European Transaction on Electrical Power*, vol. 5, no. 3, pp. 359–366, Jan. 1993.
- [7] A. Stankovic, M. Ilic, and D. Maratukulam, "Recent results in secondary voltage control of power systems," *Power Systems, IEEE Transactions on*, vol. 6, no. 1, pp. 94 –101, Feb. 1991.
- [8] T. Amraee, A. M. Ranjbar, and R. Feuillet, "Immune-based selection of pilot nodes for secondary voltage control," *European Transaction on Electrical Power Engineering*, vol. X, no. e7377, p. 114, Jan. 2009.
- [9] B. Marinescu and H. Bourles, "Robust predictive control for the flexible coordinated secondary voltage control of large-scale power systems," *Power Systems, IEEE Transactions on*, vol. 14, no. 2, p. 12621268, May 1999.
- [10] A. C. R. Llorenz, J. Tapia and J. M. Grijalba, "Secondary voltage control based on a robust multivariable pi controller," in *Proc. 11th PSCC, Avignon, France, 1993*, 12-14 1994, p. 10111018.
- [11] H. F. Wang, "Multi-agent co-ordination for the secondary voltage control in power system contingencies," in *Proc. Inst. Elect. Eng. C, 2001*, 12-14 2001, p. 6166.
- [12] H. F. Wang, H. Li, and H. Chen, "Coordinated secondary voltage control to eliminate voltage violations in power system contingencies," *Power Systems, IEEE Transactions on*, vol. 18, no. 2, pp. 588 – 595, May 2003.
- [13] S. Corsi, "Wide area voltage protection," *Generation, Transmission Distribution, IET*, vol. 4, no. 10, pp. 1164 –1179, October 2010.
- [14] E. Vaahedi, C. Fuchs, W. Xu, Y. Mansour, H. Hamadanizadeh, and G. Morison, "Voltage stability contingency screening and ranking," *Power Systems, IEEE Transactions on*, vol. 14, no. 1, pp. 256 –265, Feb. 1999.
- [15] S. Pineda and A. Conejo, "Scenario reduction for risk-averse electricity trading," *Generation, Transmission Distribution, IET*, vol. 4, no. 6, pp. 694 –705, 2010.
- [16] J. Morales, S. Pineda, A. Conejo, and M. Carrion, "Scenario reduction for futures market trading in electricity markets," *IEEE Trans. on Power Sys.*, vol. 24, no. 2, pp. 878 –888, May 2009.
- [17] A. P. Engelbrecht, *Computational Intelligence : An Introduction*. University of Pretoria South Africa: JHON WILEY & SONS, 2007.
- [18] A. Soroudi and M. Ehsan, "A distribution network expansion planning model considering distributed generation options and techno-economical issues," *Energy*, vol. 35, no. 8, pp. 3364 – 3374, 2010.
- [19] A. Soroudi, M. Ehsan, and H. Zareipour, "A practical eco-environmental distribution network planning model including fuel cells and non-renewable distributed energy resources," *Renewable Energy*, vol. 36, no. 1, pp. 179 – 188, 2011.
- [20] D. Floreano and C. Mattiussi, *Bio-Inspired Artificial Intelligence: Theories Methods and Technologies*. The MIT Press, 2008.
- [21] J. Fulcher and L. C. Jain, *Computational Intelligence: A Compendium*. Springer, 2008.
- [22] Y. Atwa and E. El-Saadany, "Probabilistic approach for optimal allocation of wind-based distributed generation in distribution systems," *Renewable Power Generation, IET*, vol. 5, no. 1, pp. 79 –88, 2011.
- [23] A. Conejo, J. de la Fuente, and S. Goransson, "Comparison of alternative algorithms to select pilot buses for secondary voltage control in electric power networks," in *Electrotechnical Conference, 1994. Proceedings., 7th Mediterranean*, 12-14 1994, pp. 940 –943 vol.3.
- [24] A. J. Conejo, M. Carrion, and J. M. Morales, *Decision Making Under Uncertainty in Electricity Markets*. New York: Springer, 2010.